# Melting behavior of H₂O at high pressures and temperatures

Jung-Fu Lin,[1] Eugene Gregoryanz,[1] Viktor V. Struzhkin,[1] Maddury Somayazulu,[1,2] Ho-kwang Mao,[1] and Russell J. Hemley[1]

[1] Water plays an important role in the physics and chemistry of planetary interiors. In situ high pressure-temperature Raman spectroscopy and synchrotron x-ray diffraction have been used to examine the phase diagram of H₂O. A discontinuous change in the melting curve of H₂O is observed at approximately 35 GPa and 1040 K, indicating a triple point on the melting line. The melting curve of H₂O increases significantly above the triple point and may intersect the isentropes of Neptune and Uranus. Solid ice could therefore form in stratified layers at depth within these icy planets. The extrapolated melting curve may also intersect with the geotherm of Earth's lower mantle above 60 GPa. The presence of solid H₂O would result in a jump in the viscosity of the mid-lower mantle and provides an additional explanation for the observed higher viscosity of the mid-lower mantle. **Citation:** Lin, J.-F., E. Gregoryanz, V. V. Struzhkin, M. Somayazulu, H.-k. Mao, and R. J. Hemley (2005), Melting behavior of H₂O at high pressures and temperatures, *Geophys. Res. Lett.*, *32*, L11306, doi:10.1029/2005GL022499.

## 1. Introduction

[2] The properties and phase relations of H₂O at high pressures and temperatures (*P-T*) are important to geophysical, physical, and planetary problems. Recent studies have expanded our understanding of the polymorphism in H₂O at high pressures and at modest temperatures (300 K and below up to 100 GPa). The flexibility of hydrogen bonding in the system gives rise to myriad phases (some 15) including stable and metastable crystalline and amorphous (and possibly liquid) phases. All of those phases observed below 60 GPa have structures dictated by the ice rules [*Pauling*, 1935]. At higher pressures, symmetrization of the hydrogen-bonded network occurs, forming an ionic state, ice X. This transition was originally predicted from crystal chemical arguments and subsequently by calculations before being realized experimentally [*Aoki et al.*, 1996; *Goncharov et al.*, 1996]. Theoretical calculations have predicted the existence of other symmetrically hydrogen-bonded phases at higher pressures based on denser packing of the oxygen sublattice [*Benoit et al.*, 1996].

[3] There has been comparatively little direct information on the behavior of H₂O at high *P-T* (e.g., above 300 K at tens of gigapascals). This regime is crucial for modeling planetary interiors and for identifying and understanding numerous chemical reactions at extreme conditions [*Scott et al.*, 2002]. In particular, under extreme *P-T* conditions, fluid water changes from hydrogen-bonded to dissociation dominated, as suggested by shock-wave experiments and first-principles simulations [*Holmes et al.*, 1985; *Schwegler et al.*, 2001]. Intriguing high-temperature behavior for the dense H₂O solid has also been predicted by first-principles calculations; specifically, a superionic phase of ice VII has been proposed involving a molten hydrogen-bonded sublattice with the oxygen sublattice remaining in a body-centered cubic (bcc) arrangement [*Cavazzoni et al.*, 1999]. There have been a few direct measurements to explore this high *P-T* behavior [*Fei et al.*, 1993; *Datchi et al.*, 2000; *Dubrovinskaia and Dubrovinsky*, 2003; *Lin et al.*, 2004; *Schwager et al.*, 2004]. A comparison of the predicted transition temperature with melting measurements shows that the superionic regime is predicted to occur at a significantly higher temperature than the extrapolated melting lines, with the low *P-T* boundary of this regime estimated to be around 30 GPa and 1450 K [*Cavazzoni et al.*, 1999]. Although conflicting reports of the melting curve of H₂O have been resolved in recent studies using high *P-T* Raman spectroscopy to 22 GPa and 900 K [*Lin et al.*, 2004], a significantly higher melting line with a discontinuous change at approximately 43 GPa and 1600 K has been reported at higher pressures [*Schwager et al.*, 2004]. Here we used high *P-T* diamond anvil cells (DAC) for in situ Raman and x-ray diffraction measurements to 60 GPa and 1300 K in order to explore the higher *P-T* behavior of H₂O and D₂O.
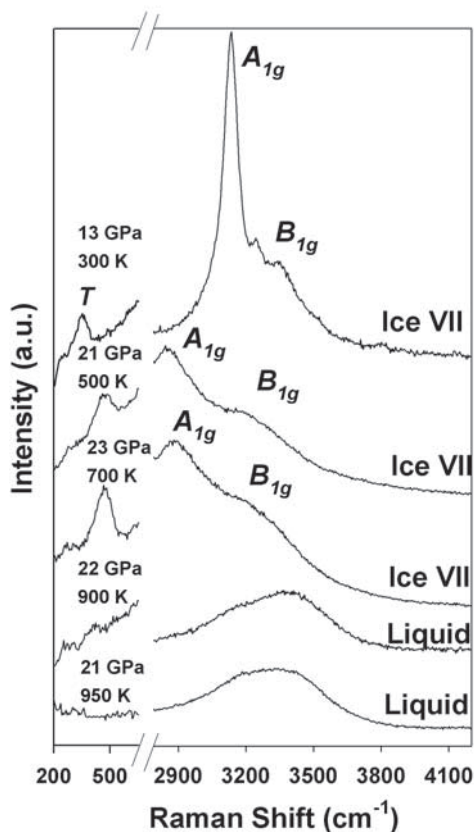
## 2. Experiments

[4] Distilled and deionized H₂O or D₂O (99.9%) was loaded into ~100 μm diameter and ~20 μm thick sample chambers in the high-temperature DACs, which were equipped with two resistive heaters and thermocouples [*Fei et al.*, 1993; *Lin et al.*, 2004; *Bassett et al.*, 1993]. Various metal gaskets and Nd:YLF laser absorbing metals have also been used to test for potential chemical reactions with H₂O in an externally-heated DAC (EHDAC) (Re gasket; W, Ir, or Au gasket insert in Re gasket) or in a laser-heated DAC (LHDAC) [*Santoro et al.*, 2004a] (thin Pt or W laser absorber in Re gasket; thin Ir laser absorber in Ir gasket insert (in Re gasket)). Sm:YAG, loaded in a separate hole close to the sample chamber, was used as the pressure calibrant because its fluorescence remains strong at high temperature. Since the pressure calibrant was not placed in the sample chamber, test experiments were performed by placing Sm:YAG and ruby chips in both chambers up to ~650 K to correct the pressure difference which was about 10% [*Lin et al.*, 2004]. The spectroscopic measurements of pressure were supplemented by observa-
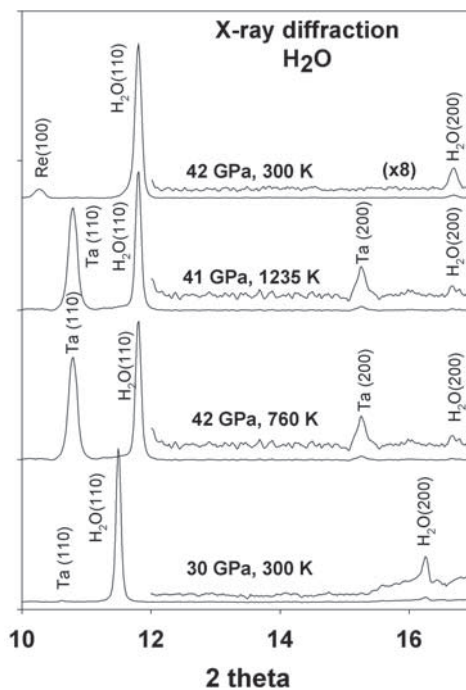
---

[1]Geophysical Laboratory, Carnegie Institution of Washington, Washington, D. C., USA.

[2]High Pressure Collaborative Access Team, Advanced Photon Source, Argonne National Laboratory, Argonne, Illinois, USA.

tions of the pressure shift of the high frequency edge of the first-order Raman band from the diamond anvil, as well as by measurements of the ruby fluorescence at lower temperature. The temperature was measured to within ±1 K below 600 K and ±5 K above 600 K in EHDAC experiments. Raman spectra were measured using standard lines (e.g., 514.5, 487.9 nm) of Ar$^+$ lasers with custom built micro-optical systems consisting of a single-stage 460 mm spectrograph, liquid nitrogen-cooled CCD, and notch filters. Angle-dispersive x-ray diffraction was measured at beam-line 16-ID-B, HPCAT of the Advanced Photon Source (APS). Monochromatic x-ray beams were focused down to ∼10 μm and the diffracted x-rays were recorded with a CCD calibrated with a CeO$_2$ standard. During the diffraction experiments, the equations of state of tantulum (Ta),



**Figure 2.** Angle-dispersive x-ray diffraction patterns of the H$_2$O sample at high *P-T*. A monochromatic beam (wavelength = 0.4157 Å) was used as the x-ray source and the diffracted x-rays were collected by a CCD (MARCCD). Amorphous BN was used as the diamond seat to allow a wider diffraction angle. Tantalum (Ta) was used as an internal pressure calibrant because of its inertness and simple bcc structure. The equation of state of ice VII was also used to determine the pressure in situ [*Fei et al.*, 1993].
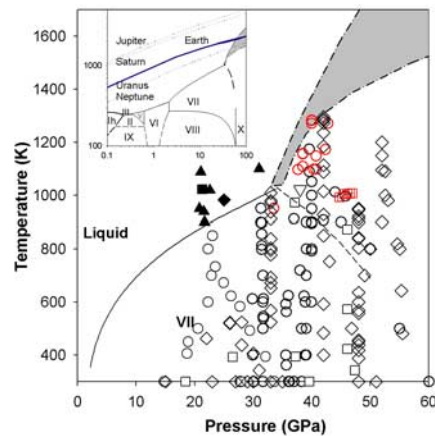


**Figure 1.** Representative Raman spectra of H$_2$O at high *P-T*. The Raman-active OH-stretching bands and the translational modes of H$_2$O are used to detect melting. The translational mode is observed in solid ice VII whereas it disappears in liquid H$_2$O. The OH-stretching modes change significantly across melting; the low-frequency A$_{1g}$ mode is the dominant band in ice VII while the high-frequency mode dominates in liquid water. *T*: translational mode. The OH-stretching modes overlap with the second-order Raman signal from the diamond anvils at pressure above ∼25 GPa, making it difficult to use these modes to detect melting. The spectra of the translational mode can still be used to detect melting (see supplementary materials for details).

gold (Au) and ice VII were used to determine pressure [*Fei et al.*, 1993].

## 3. Results and Discussion

[5] We have used the Raman-active OH-stretching bands, the translational modes, optical observations of melting features, and x-ray diffraction of the oxygen bcc sublattice to detect melting in H$_2$O up to 60 GPa and 1300 K in an EHDAC. Our results show that the frequencies and the intensities of the OH-stretching peaks change significantly across the melting line, the translational mode disappears in the liquid phase (Figure 1), and the observation of the sharp x-ray diffraction peaks indicates the presence of the oxygen bcc sublattice in H$_2$O (Figure 2). These observations are consistent with the optical detection of melting features. The observed melting curve below 35 GPa is in accord with our previous study [*Lin et al.*, 2004]; however, a discontinuous change in the melting curve of H$_2$O occurs at approximately 35 GPa and 1040 K (Figure 3). Along the melting line above 35 GPa, in situ high *P-T* Raman measurements on H$_2$O reveal two strong Raman peaks in the region of 200-700 cm$^{-1}$ and one peak at ∼1600 cm$^{-1}$. The additional peaks were distinct from all known phases of ice (i.e., ice VII, ice VIII, and ice X) but consistent with those of ε-O$_2$ [*Santoro et al.*, 2004b] (see

supplementary materials[1] for details). The presence of a small amount of $O_2$ was further confirmed by decompressing the sample to below the ε-β transition of $O_2$, observing the disappearance of ε-$O_2$-like Raman peaks, and splitting of the Raman band at ~600 cm$^{-1}$ at approximately 60 GPa. The ε-$O_2$-like Raman peaks are observed using Re, W, and Au gasket insert in EHDAC experiments or Pt, W, and Ir metal laser absorber in LHDAC experiments, indicating that $H_2O$ reacts with all gasket metals examined to form metal hydrides. The formation of $O_2$ arises from loss of hydrogen to the gasket or metal laser absorber because there was no evidence for free $H_2$ or $D_2$, which are characterized by a very intense Raman vibron [*Gregoryanz et al.*, 2003]. The facile loss of hydrogen from the sample may explain the reports of dissociation of $H_2O$ in previous LHDAC experiments [*Benedetti et al.*, 2001]. The observation of sudden hydrogen loss above the melting slope discontinuity at 35 GPa is consistent with the localized-itinerant transition of hydrogen, associated with the transformation from ice VII to the higher pressure phase.

[6] Additional information on the melting behavior of $H_2O$ was obtained using in situ synchrotron x-ray diffraction measurements on $H_2O$ up to 45 GPa and 1300 K. Angle-dispersive x-ray diffraction patterns of the $H_2O$ sample showed diffraction peaks of the oxygen atoms in a bcc sublattice (Figures 2 and 3). Combining these results with the in situ Raman study, it is evident that $H_2O$ remains in the solid phase above the extrapolated melting curves from previous studies [*Lin et al.*, 2004] and that a discontinuous change in the melting line occurs at approximately 35 GPa and 1040 K. The exact location of the melting curve at higher *P-T* conditions remains to be determined in the future as the melting temperature of $H_2O$ above 40 GPa is beyond the temperature capability of the conventional EHDAC techniques. The change of the melting is independent of the observation of the ε-$O_2$ and indicates that a first-order transition occurs at these high *P-T* conditions. From optical observations in a LHDAC, a distinct change in melting slope of $H_2O$ at about 43 GPa and 1600 K has been suggested as a first-order transformation from ice VII to ice X, though the melting curve was much higher than all other studies [*Schwager et al.*, 2004]. Recent in situ high *P-T* Raman measurements of solid $CO_2$ in a LHDAC showed that the sample temperature was lower than the surface temperature when a metallic laser coupler is used [*Santoro et al.*, 2004a]; these results suggest that the melting curve reported by *Schwager et al.* [2004] should be corrected further downward. The phase transition between ice VII and ice X begins at 60 GPa and 300 K [*Goncharov et al.*, 1999]. The extension of the boundary with a negative Clapeyron slope can explain the triple point at approximately 35 GPa and 1040 K. The observed discontinuous change in the melting curve also occurs in the general *P-T* region predicted for the superionic phase [*Cavazzoni et al.*, 1999]. The extra degrees of freedom of the protons would add to the entropy of the superionic phase and therefore, substantially raise the melting temperature of the system. The extent to which the increase in the melting temperature is associated with higher intrinsic entropy of the



**Figure 3.** High *P-T* phase diagram of $H_2O$. Black solid line, extrapolated melting curve of ice VII [*Lin et al.*, 2004]; open circles, solid $H_2O$ (Raman and optical observation); solid triangles up: liquid in $H_2O$ (Raman and optical observation); open diamond: solid ice (x-ray diffraction); open square: solid $D_2O$ (Raman and optical observation); solid square: liquid $D_2O$ (Raman and optical observation); open triangle down: liquid $H_2O$ (optical observation only); solid diamond: liquid $H_2O$ (optical observation and x-ray diffraction); red open circles and squares, observation of ε-$O_2$ in $H_2O$ and $D_2O$ (Raman), respectively; dash-dot line and grey area: upper bound and lower bound of the extrapolated melting curve; dash line: schematic phase boundary in solid $H_2O$. The upper bound is extrapolated assuming a rather continuous increase in the melting line whereas a turnover of the melting curve gives rise to the extrapolated lower bound. An increase in melting temperature of $H_2O$ is expected at around 35 GPa and 1040 K.; though, precise location of the melting curve above the triple point remains to be determined in the future. We note that the observation of the ε-$O_2$ peaks is not used to determine the discontinuous change of the melting curve. Since a discontinuous change in the melting curve of $H_2O$ indicates a triple point on the melting line, the schematic phase boundary in solid $H_2O$ could be due to either the extension of the phase transformation from ice VII to ionic ice X at 60–80 GPa and 300 K [*Goncharov et al.*, 1999] or the occurrence of the theoretically predicted superionic phase [*Cavazzoni et al.*, 1999]. Insert: proposed new phase diagram of $H_2O$; dotted lines: isentropes in Jupiter, Saturn, Uranus, and Neptune [*de Pater and Lissauer*, 2001], respectively; blue solid line: geotherm [*Brown and Shankland*, 1981].

high pressure solid phase, a pre-melting effect in that phase, or the actual formation of a distinct superionic phase remains to be determined.

## 4. Planetary and Geophysical Applications

[7] The steep increase in the melting curve of $H_2O$ at high *P-T* conditions has important implications for planetary interiors. $H_2O$ is believed to be a major component of the intermediate ice layers in the interiors of Uranus and Neptune [*Nellis et al.*, 1988; *Hubbard et al.*, 1991]. Depending on the curvature of the extrapolated melting curve above 35 GPa, the melting curve may intersect proposed isen-

---

[1]Auxiliary material is available at ftp://ftp.agu.org/apend/gl/2005GL022499.

tropes of Neptune and Uranus above 50 GPa (Figure 3) [*de Pater and Lissauer*, 2001]. The high *P-T* solid phase may thus form stratified icy layers at depth within these planets. From the Clausius-Clapeyron equation ($dT/dP = \Delta V/\Delta S$), the steep increase in the melting curve above 35 GPa indicates a likely large change in $\Delta V/\Delta S$, suggesting a significant change in physical properties of $H_2O$ above the triple point. The change in the melting curve of $H_2O$ and in the mobility of hydrogen also affects the electrical properties and the pressure-density distribution within these icy planets. The observed chemical reaction of $H_2O$ with other materials at high *P-T* is also likely to occur in nature and such reactions can also enhance chemical reactivity with $CH_4$, $NH_3$, and core forming metals to produce more complex compounds in the interiors of icy planets.

[8] There are important implications for the Earth's interior as well. Based on the water content of ordinary chondritic meteorites, it is believed that two-thirds of Earth's original $H_2O$ has either been lost to space or is locked in the deep interior. Based on the extrapolated melting curve of ice VII [*Datchi et al.*, 2000], it has been suggested that ice VII exists in portions of the coldest subducting slabs after water is liberated from hydrous minerals by successive dehydration processes [*Bina and Navrotsky*, 2000]. Our extrapolated melting curve above 35 GPa could intersect with the much hotter geotherm of the lower mantle (~60 GPa) (Figure 3) [*Brown and Shankland*, 1981]. Thus, $H_2O$ could be in solid form below 1600 km in depth. Based on seismic and geodynamic data, a high-viscosity layer with strongly suppressed flow-induced deformation and convective mixing has been proposed to exist near 2000 km depth [*Forte and Mitrovica*, 2001]. The existence of solid ice suggests a jump in viscosity within the mid-lower mantle and provides an additional explanation for its viscosity heterogeneity. On the other hand, the ascending deep mantle plumes would give rise to melting of $H_2O$ in the hot mantle materials, supporting the hypothesis that hot spots could also be wet spots [*Schilling et al.*, 1980]. Our results show that $H_2O$ reacts with even nominally unreactive refractory metals. The reaction of $H_2O$ with core forming metals such as iron to form metal hydrides (i.e., $FeH_x$ + FeO) provides a mechanism for incorporation of hydrogen into growing planetary cores [*Williams and Hemley*, 2001].

## References

Aoki, K., H. Yamawaki, M. Sakashita, and H. Fujihisa (1996), Infrared absorption study of the hydrogen-bond symmetrization in ice to 110 GPa, *Phys. Rev. B*, 54, 15,673–15,677.

Bassett, W. A., A. H. Shen, M. Bucknum, and I. M. Chou (1993), A new diamond anvil cell for hydrothermal studies to 10 GPa and −190°C to 1100°C, *Rev. Sci. Instrum.*, 64, 2340–2345.

Benedetti, L., et al. (2001), Water in planets: Dissociation of $H_2O$ at high pressures and temperatures to a new form of oxygen, *Eos Trans. AGU*, 82(47), Fall Meet. Suppl., Abstract V51A-0977.

Benoit, M., M. Bernasconi, P. Focher, and M. Parrinello (1996), New high-pressure phase of ice, *Phys. Rev. Lett.*, 76, 2934–2936.

Bina, C. R., and A. Navrotsky (2000), Possible presence of high-pressure ice in cold subducting slabs, *Nature*, 408, 844–847.

Brown, J. M., and T. J. Shankland (1981), Thermodynamic parameters in the Earth as determined from seismic profiles, *Geophys. J. R. Astron. Soc.*, 66, 579–596.

Cavazzoni, C., et al. (1999), Behavior of ammonia and water at high pressure and temperature: Implications for planetary physics, *Science*, 283, 44–46.

Datchi, F., P. Loubeyre, and R. LeToullec (2000), Extended and accurate determination of the melting curves of argon, helium, ice ($H_2O$), and hydrogen ($H_2$), *Phys Rev. B*, 61, 6535–6546.

de Pater, I., and J. J. Lissauer (2001), *Planetary Sciences*, Cambridge Univ. Press, New York.

Dubrovinskaia, N., and L. Dubrovinsky (2003), Melting curve of water studied in externally heated diamond-anvil cell, *High Pressure Res.*, 23, 307–310.

Fei, Y., H. K. Mao, and R. J. Hemley (1993), Thermal expansivity, bulk modulus, and melting curve of $H_2O$-ice VII to 20 GPa, *J. Chem. Phys.*, 99, 5369–5373.

Forte, A. M., and J. X. Mitrovica (2001), Deep-mantle high-viscosity flow and thermochemical structure inferred from seismic and geodynamic data, *Nature*, 410, 1049–1056.

Goncharov, A. F., V. V. Struzhkin, M. Somayazulu, R. J. Hemley, and H. K. Mao (1996), Compression of $H_2O$ ice to 210 GPa: Evidence for a symmetric hydrogen-bonded phase, *Science*, 273, 218–220.

Goncharov, A. F., V. V. Struzhkin, H. K. Mao, and R. J. Hemley (1999), Raman spectroscopy of dense ice and the transition to symmetric hydrogen bonds, *Phys. Rev. Lett.*, 83, 1998–2001.

Gregoryanz, E., A. F. Goncharov, K. Matsuishi, H. K. Mao, and R. J. Hemley (2003), Raman spectroscopy of hot dense hydrogen, *Phys. Rev. Lett.*, 90, 175701.

Holmes, N. C., W. J. Nellis, W. B. Graham, and G. E. Walrafen (1985), Spontaneous Raman scattering from shocked water, *Phys. Rev. Lett.*, 55, 2433–2436.

Hubbard, W. B., et al. (1991), Interior structure of Neptune: Comparison with Uranus, *Science*, 253, 648–651.

Lin, J. F., et al. (2004), High pressure-temperature Raman measurements of $H_2O$ melting to 22 GPa and 900 K, *J. Chem. Phys.*, 121, 8423–8427.

Nellis, W. J., et al. (1988), The nature of the interior of Uranus based on studies of planetary ices at high dynamic pressure, *Science*, 240, 779–781.

Pauling, L. (1935), Structure and entropy of ice and of other crystals with some randomness of atomic arrangement, *J. Am. Chem. Soc.*, 57, 2680–2684.

Santoro, M., J. F. Lin, H. K. Mao, and R. J. Hemley (2004a), In situ high *P-T* Raman spectroscopy and laser heating of carbon dioxide, *J. Chem. Phys.*, 121, 2780–2787.

Santoro, M., E. Gregoryanz, H. K. Mao, and R. J. Hemley (2004b), New phase diagram of oxygen under high pressures and high temperatures, *Phys. Rev. Lett.*, 93, 265701.

Schilling, J. G., M. B. Bergeron, and R. Evans (1980), Halogens in the mantle beneath the North Atlantic, *Philos. Trans. R. Soc. London, Ser. A*, 297, 147–178.

Schwager, B., L. Chudinovskikh, A. Gavriluk, and R. Boehler (2004), Melting curve of $H_2O$ to 90 GPa measured in a laser-heated diamond cell, *J. Phys. Condens. Matter*, 16, S1177–S1179.

Schwegler, E., G. Galli, F. Gygi, and R. Q. Hood (2001), Dissociation of water under pressure, *Phys. Rev. Lett.*, 87, 265501.

Scott, H. P., Q. Williams, and F. J. Ryerson (2002), Experimental constraints on the chemical evolution of large icy satellites, *Earth Planet. Sci. Lett.*, 203, 399–412.

Williams, Q., and R. J. Hemley (2001), Hydrogen in the deep Earth, *Annu. Rev. Earth Planet. Sci.*, 29, 365–418.

————————

E. Gregoryanz, R. J. Hemley, J.-F. Lin, H.-k. Mao, and V. V. Struzhkin, Geophysical Laboratory, Carnegie Institution of Washington, 5251 Broad Branch Rd., Washington, DC 20015, USA. (j.lin@gl.ciw.edu)

M. Somayazulu, HPCAT, Advanced Photon Source, Argonne National Laboratory, Argonne, IL 60439, USA.